IEEE Journal of Translational Engineering in Health and Medicine

Received 21 August 2013; revised 18 November 2013 and 28 January 2014; accepted 15 March 2014.
Date of publication 8 April 2014; date of current version 22 April 2014.

Digital Object Identifier 10.1109/JTEHM.2014.2316148

Urine Flow Dynamics Through Prostatic Urethra With Tubular Organ Modeling Using Endoscopic Imagery

TAKURO ISHII[1], (Student Member, IEEE), YOICHI KAMBARA[1], TOMONORI YAMANISHI[2], YUKIO NAYA[3], AND TATSUO IGARASHI[4]

[1]Graduate School of Engineering, Chiba University, Chiba 263-8522, Japan
[2]Department of Urology, Dokkyo Medical University, Tochigi 321-0293, Japan
[3]Department of Urology, Teikyo University Chiba Medical Center, Chiba 299-0111, Japan
[4]Center for Frontier Medical Engineering, Chiba University, Chiba 263-8522, Japan

CORRESPONDING AUTHOR: T. Ishii (taku_ishii@graduate.chiba-u.jp)

This work was supported by the Japan Society for the Promotion of Science KAKENHI under Grant 23659753 and Grant 24·358.

ABSTRACT Voiding dysfunction is common in the aged male population. However, the obstruction mechanism in the lower urinary tract and critical points for obstruction remains uncertain. The aim of this paper was to develop a system to investigate the relationship between voiding dysfunction and alteration of the shape of the prostatic urethra by processing endoscopic video images of the urethra and analyzing the fluid dynamics of the urine stream. A panoramic image of the prostatic urethra was generated from cystourethroscopic video images. A virtual 3-D model of the urethra was constructed using the luminance values in the image. Fluid dynamics using the constructed model was then calculated assuming a static urethra and maximum urine flow rate. Cystourethroscopic videos from 11 patients with benign prostatic hyperplasia were recorded around administration of an alpha-1 adrenoceptor antagonist. The calculated pressure loss through the prostatic urethra in each model corresponded to the prostatic volume, and the improvements of the pressure loss after treatment correlated to the conventional clinical indices. As shown by the proposed method, the shape of the prostatic urethra affects the transporting urine fluid energy, and this paper implies a possible method for detecting critical lesions responsible for voiding dysfunction. The proposed method provides critical information about deformation of the prostatic urethra on voiding function. Detailed differences in the various types of relaxants for the lower urinary tract could be estimated.

INDEX TERMS Benign prostatic hyperplasia, cystourethroscopy, computational biophysics, computer-aided diagnosis, endoscopes, fluid dynamics, less invasive therapy, voiding dysfunction.

I. INTRODUCTION

The number of patients suffering from voiding dysfunction is common among aged population in male. Preservation of comfortable urination together with continence is a mainstay of a fair quality of life (QOL). Conventionally, voiding function is evaluated by various methods. Scoring symptoms is simple and widely adopted to estimate subjective seriousness. The urodynamics study (UDS) provides physiological estimation of lower urinary tract function, however, requires transurethral insertion of a catheter into the bladder to infuse isotonic water and to measure the intraluminal pressure of the bladder and rectum. The assessment of the volume of residual urine (RU) and excreted urine also has been accepted in clinical practice, and provides objective parameters of patients' voiding function. However, urination is integration of the neurologic reflexes, motion of smooth muscles of the lower urinary tracts, and hydraulic effects of non-turbulent urine flow in the urethra that UDS cannot cover with sufficient accuracy.

The shape deformation of the prostatic urethra is a potent factor contributing to voiding dysfunction. Benign prostatic hyperplasia (BPH) [1], [2] and bladder outlet

obstruction (BOO) are known as the major causes of voiding dysfunction, where alteration of the intraluminal shape and/or elasticity is observed in the prostatic urethra. However, there have been sparse attempts to clarify the relationship between the change in shape of the luminal cavity of the prostatic urethra and the urinary flow by mathematical model [3], despite the knowledge that relaxation of smooth muscle of the urethra or surgical dilation improves the urine stream. Thus, there is a lack of methods for estimating the urine flow in the urethra, which makes formulating therapeutic strategies difficult and their outcome somewhat uncertain. To improve treatment outcome and to offer methods to select an optimal therapy in each patient, detailed understanding of the alteration in shape of the prostatic urethra and intraluminal behavior of urine is essential.

The computational fluid dynamics (CFD) was considered as a possible way to predict intra-urethral flow behavior, and reconstruction of the prostatic urethra is a critical issue. Imaging modalities such as computerized tomography (CT) [4], magnetic resonance imaging (MRI) [5], [6] and ultrasonography [7], [8] seem to be inadequate to extract sufficient three-dimensional (3D) information of the intraluminal cavity of the prostatic urethra accurately enough to calculate the flow dynamics of urine. Besides, image acquisition using CT or MRI is not practical because of extra-ordinal voiding condition for the patients and limitations of time- and spatial-resolution of the apparatuses. In contrast, endoscopy could be a useful method for precisely constructing the 3D shape of the prostatic urethra [9]–[11]. During cystourethroscopy, the urinary tract is filled with irrigant set at a pressure of 80 cm H_2O, which opens and cleans the prostatic urethra and the bladder, enabling optimal observation of the tract with reproducibility.

In a previous study, we introduced a method to generate panoramic images and 3D models with texture information of the intraluminal surface of tubular organs using conventional single-lens endoscopic imagery, and tested it on two types of dummy model with an endoscope fixed on the linear stage [12]. Because endoscopic imagery fails to cover multi-angle and wide-range observation when inserted in narrow spaces, panoramic or virtual 3D images would intuitively depict comprehensive structures of organs. The shape of the constructed model and the ratio of the height of the bump set in the pipe was confirmed to be comparable to the actual height [12]. In addition, the resolving power to depict anatomical features in a luminal organ of the method was validated using a porcine colon by comparing the constructed model with the resected organ [12]. The reproducibility of the panoramic image with different video sources from the same subject was validated in another short report [13].

In this paper, we applied modeling of the intraluminal surface of a tubular organ to the solid model construction of the expanded urethra at approximately the maximum flow rate for CFD analysis, which visualizes fluid behavior through the urethra, to analyze the physical properties of voiding dysfunction. The idea originated from experimental [14], [15] and computational analyses [16]–[18] of urine flow dynamics through the urethra of patients with BPH and BOO, which suggested the diffuser-like shape in the urethra generated by the obstruction would cause large vortex flow in the urethra and fluid energy loss. Though the method [12] generates the relative size and shape of the luminal organ from the endoscopic video, the CFD using the constructed model may indicate the local urine behavior that cause abnormal fluid energy loss in individual patient.

In the following section, we describe a method to construct a 3D model of the prostatic urethra from an endoscopic video, using the cystourethroscope as the scanner. The urine flow through the prostatic urethra was subsequently visualized and analyzed the efficiency of urine transportation in the urethra. Finally, 22 cystourethroscopic videos recorded during clinical practice, under approval of the local ethics committee and with informed consent of patients, were processed with the proposed method and the relationships between and differences from conventional UDS data were discussed.

II. METHODS AND PROCEDURES

To extract continuous surface information of color and shape, the conventional cystourethroscope was withdrawn from the bladder outlet through the prostatic urethra to the external urethral sphincter under constant pressure of irrigant at a constant velocity, angle and axis [10] for approximately 10 seconds. The video images from the cystourethroscope were recorded during the scanning movement and were captured in VGA resolution. Cystourethroscope motion has two degrees of freedom; longitudinal and rotational. Compared to other tubular organs, such as the colon, the shape of the prostatic urethra is narrow and rather smooth, which would avoid the optical occlusion during the scanning. The procedure consisted of three steps. In the first step, the recorded images were made into a panoramic image [10]. In the second step, modeling methods were used to calculate the shape of the intraluminal urethra based on luminance values [12]. In the last step, a CFD method [16], [17], [19], [20] was used to simulate the streamline of the virtual urine flow and the fluid energy transition along the urinary tract.

A. MODELING OF INTRALUMINAL SURFACE OF URETHRA USING ENDOSCOPIC IMAGERY

The shape modeling method used to obtain the urethral surface shape for the urine flow analysis is a luminance-based shape extraction method specialized for the narrow spaces encountered during endoscopy [10], [12]. This method provides simultaneous observation of the shape and color of the intraluminal tissue. The first step is capturing texture information of the intraluminal surface of recorded tissue along the trajectory of the endoscope. The method of generating the panoramic image for endoscopic images of the luminal tissue proposed by Igarashi et al. [10] was used.

In brief, an opened panoramic image was generated by using the cystourethroscope as a scanner of the luminal object following the endoscopic movement. At first, a circle was

IEEE Journal of Translational Engineering in Health and Medicine

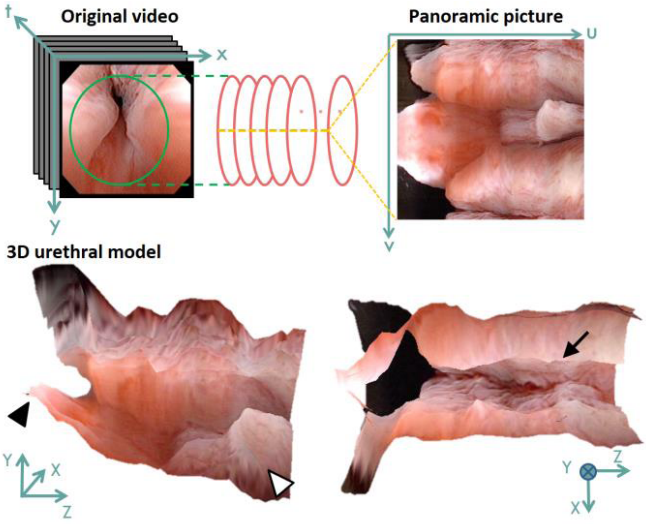

FIGURE 1. Schematic showing processing of the 3D model of the urinary tract. Closed and opened triangles and arrow indicate the bladder outlet, verumontanum and protruded prostate respectively, which are the remarkable anatomical features of urethra. (Left: sagittal cross section; Right: coronal cross section of a constructed model).

depicted on a video frame by the operator to determine the center axis and radius of the scanning line for generating the panoramic image (Fig. 1). The relationship between the pixels in a video stream and those of a panoramic image can be described as,

$$P(u, v) = V_u(r \sin \frac{v}{r} + c_x, r \cos \frac{v}{r} + c_y) \tag{1}$$

where $P(u, v)$ and $V_t(x, y)$ are a pixel of a panoramic image and a video frame at time t, respectively. c_x, c_y and r are the selected center point and radius of the selected circle for scanning.

In endoscopy, the intraluminal cavity of the prostatic urethra was expanded by the endoscope itself and the expansion was reduced just after withdrawal, and balanced with dynamic pressure of the irrigant.

Here, we assumed the endoscopic optical environment; 1: a single point light source with a coaxial image sensor, 2: uniform reflection characteristics in the individual urethral tissue, and 3: lambertian reflection surface. In addition, though the endoscope tend to have strong optical distortions, since the center point of the scanning circle was placed at the optical axis of the endoscope and pixels on the circle were retrieved for the processing, the distortion effect was negligible under the radical distortion model. Then, the relative distance between tip of the endoscope and a point of a urethra was described with the inverse-square law of luminance as,

$$L = (\alpha \frac{k_d \cdot I_q}{R^2} \cos \theta)^{\gamma} \tag{2}$$

where L is the observed intensity value of each pixel, k_d is the reflection coefficient, which is unique under the second assumption aforementioned, I_q is the intensity of illumination of endoscope, which is constant during a video recording, θ is an angle of incidence of a ray, R is the distance between a point of an object and the camera, γ is the gamma value of the image processor of the cystourethroscope, and α is a constant. Then, the relative distance between the optical axis of the camera and a point in a urethra contained in a panoramic image could be described as,

$$R(u, v) = k \sqrt{\frac{\cos \theta}{L(u, v)^{(\gamma^{-1})}}} \tag{3}$$

where $L(u, v)$ and $R(u, v)$ indicate a luminance value and relative distance to the object of a pixel on $P(u, v)$, respectively. k is an optional constant ($0<k<1$).

In (3), $\cos\theta$ could be regarded as constant because the distance between the surface and the camera is very short and the shape variation is restricted to within a few degrees. In addition, R was immediately decreased within small values of $L(u, v)$ and the relationship between $R(u, v)$ and $L(u, v)$ indicated approximately linearity at most frequent range of the intensity value. Thus, the relative distance between optical axis and a point of a urethra in a panoramic image were re-defined,

$$R'(u, v) = \frac{1 - L'(u, v)}{1 - L'_{\min}} \cdot w + b \tag{4}$$

$$w = \frac{D_{\max} - D_{\min}}{D_{\max}},\ b = \frac{D_{\min}}{D_{\max}} \tag{5}$$

where $R'(u, v)$ is altered relative distance. L' is luminance value after gamma correction. γ in (3) was set as 0.41 in this study. $L'_{\min}$ is minimum intensity value in a panoramic image. $D_{\max}$ and $D_{\min}$ are constants determining thickness of the model. $D_{\max}$ regulates maximum diameter of the model and size of the model. In this study, $D_{\max}$ was set at 8 mm referring to data of a healthy urethra measured by ultrasonography [21]. $D_{\min}$ regulates minimum diameter of voiding tract. Since the saturated pixels in the panoramic image interrupts CFD calculation by exaggerated obstruction, $D_{\min}$ value was set at 1 mm to continue calculation.

For each pixel in a panoramic image, we applied (4) to calculate the relative distance between a point and the optical axis. Finally, the shape of the tubular tissue was constructed by connecting points $\mathbf{S}(u,v) \in \mathbb{R}^3$ defined as,

$$S(u, v) = rR'(u, v) \begin{bmatrix} \sin \omega \\ \cos \omega \\ 0 \end{bmatrix} + \varepsilon \begin{bmatrix} 0 \\ 0 \\ u \end{bmatrix} \tag{6}$$

$$r = \frac{D_{\max}}{2},\ \omega = 2\pi \frac{v}{H},\ \varepsilon = \frac{l}{W} \tag{7}$$

where r is constant to define absolute distance, l is the length of the prostatic urethra, which was set at 25 mm, and H and W are the number of pixels in the v and u direction, respectively, in a panoramic image [12]. To our knowledge, the length of urethra l, between bladder outlet and verumontanum, had not been reported in English literature. Then, the value was estimated to be between 25 and 40 mm using MRI images of nine BPH patients who required transurethral resection

of the prostate because of enlarged prostate size and severe voiding symptom. Though we did not measure the length of the prostatic urethra in the present study, we set the length at 25 mm, a shortest length in the patients with such a severe symptom, considering the patients had moderate symptom and enlargement of prostate size managed without surgery.

Since luminal shape of major region of the prostatic urethra is rather ellipsoidal, the coefficient for depth coordinate ε should include proportionality constant to (3) in consideration of distortion of depth cue. However, as distortion in depth direction would comparably small in narrow urethral tract, as well as $\cos\theta$, the coefficient value ε was defined as (7), which covers only endoscopic movement, in this study.

Moreover, the panoramic image was placed over the corresponding location on the model to provide simultaneous shape–color observation from multiple angles (Fig. 1).

Originally, these methods [10], [12] were developed to overcome the drawbacks of endoscopic vision, such as the narrow range of view and lack of depth cue. While medical 3D imaging modalities such as CT and MRI have progressed in spatial resolution and are able to detect lesions in the body precisely, endoscopy would provide more detailed information on the intraluminal properties of the organ shown as the real color and texture of the surface, including microvasculature patterns and bleeding lesions. The opened panoramic image visualizes a wider range along the direction of endoscopic movement in the region of surface of the organ. In addition, the 3D luminal model depicts the texture information on an extracted shape model, supporting comprehension of the anatomical information.

B. CFD OF INTERNAL URINE FLOW

The tubular organ modeling depicts the 3D surface model of the prostatic urethra. Because the parts of the urethra distal to the external urethral sphincter can be regarded as a simple pipe, determining the hydraulic dynamics between the bladder side and the external urethral sphincter is essential for representing the efficiency of the urethra to transport urine. Detrusor contractility affects urine flow dynamics; however, the structural and material properties of the urethra, and how the urethra expands according to the detrusor pressure, are still challenging issues. Seeing the intraluminal space of the urethra during cystourethroscopy is dilated by equivalent normal detrusor pressure at the voiding condition with irrigant, we regarded the model processed using the method in the previous section simulates the intraluminal shape at the maximum flow rate. A rigid body and non-time-dependent fluid behavior was assumed for the fluid dynamics calculation.

The range of the original panoramic image depends on the optionally selected start and end frame, usually between the intra-bladder and distal end of the verumontanum. The width of the panoramic image depends on the velocity of the endoscope. To compare the transportation efficiency around administration of the urethral smooth muscle relaxant, a pair of panoramic images of the same patient was trimmed by setting the bladder outlet at the left side of the image and verumontanum at the right side. The left side of the trimmed image was set as the origin of the z coordinate in the modeling space. Then, all models were aligned as 25 mm in length and 4 mm in maximum radius following equation from (4) through (7), and provided constant values.

SolidWorks® Flow Simulation (Dassault Systems SolidWorks Corp.) was used for the CFD calculation and pre- and post-processing [19]. The calculation space was spatially discretized by the cut-cell method [19] with an adaptive refinement algorithm. The refinement level was determined in our previous study and set to sufficient precision for the calculation. The density and viscosity of the urine was assumed to be identical to that of water at 37 °C. Thus, the flow could be described by the incompressible Navier–Stokes equation.

$$\boldsymbol{g} - \frac{1}{\rho}\nabla p + \nu\nabla^2\boldsymbol{v} = \frac{\partial \boldsymbol{v}}{\partial t} \tag{8}$$

where, ρ, $\mathbf{g}$, p, $\boldsymbol{v}$ and ν represent density, gravitational acceleration, pressure, velocity and the coefficient of kinematic viscosity, respectively. The Navier–Stokes equation solver compiled in the SolidWorks® Flow Simulation calculated the Reynolds-averaged Navier–Stokes equation (k-ε model) by the finite volume method [19].

As aforementioned, to identify the effect of fluid energy loss caused by the shape of the urethra, the solid region was defined as rigid, and urine flow was considered constant. As the common boundary condition, boundaries between the urethral wall and fluid region were set to non-slip conditions. For the inlet condition, the total pressure was set to 104,267 Pa, following the intra-detrusor pressure at maximum urine flow during micturition of healthy people, while the outlet was exposed to atmospheric pressure, 101,325 Pa. These settings of CFD followed those of our previous reports and the simulated flow under the settings was confirmed to represent qualitatively the fluid energy loss concerning the shape of the prostatic urethra [16], [17], [22].

After the computation, as the values representing efficiency of urine transition through the model, we calculated total pressure loss between the inlet and outlet boundary (ΔP) from the total pressure (P) on a cross section defined below.

$$P = \frac{\rho}{2}\bar{v}^2 + \bar{p} \tag{9}$$

$$\Delta P = P_{in} - P_{out} \tag{10}$$

here, $\bar{v}$ and $\bar{p}$ represent mass-averaged velocity, mass-averaged pressure of the cross-section, and P_{in} and P_{out} are total pressure at the inlet boundary and outlet boundary, respectively.

In addition, to compare the alteration of transportation efficiency before and after alpha-1 adrenoceptor antagonists (alpha-1 blocker) administration, the pressure loss improvement ratio ($PLIR$) was defined as,

$$PLIR = \frac{\Delta P_{beforeTx} - \Delta P_{afterTx}}{\Delta P_{beforeTx}} \tag{11}$$

where "beforeTx" and "afterTx" indicate before and after alpha-1 blocker administration, respectively. Alpha-1 blocker

is a ''platinum'' standard and widely used for patients with urethral stricture and voiding dysfunction for relaxing the smooth muscles of the urethra. In other words, it facilitate passive deformation of the urethra from urine flow pressure provided by detrusor contraction and abdominal pressure. Therefore, after the drug has acted, the shape of the urethral wall during irrigation became smoother comparing to that before administration, and the effect would decrease shape loss of the total pressure and *PLIR* would take positive value.

C. STATISTICS

Statistical analysis was performed using Wilcoxon signed-rank test to compare means of two groups. To compute relationship between two parameters, Spearman's rank-order correlation coefficient (ρ) and p-value to test for non-correlation were used. JMP® ver.7.0.1 software (SAS Institute Inc., Cary, NC, U.S.A.) was used for calculation. Difference between two groups was considered significant when p value was less than 0.05.

III. EXPERIMENTS AND RESULTS

To examine the validity of the proposed method, cystourethroscopic videos recorded in clinical practice were processed. Sixteen pairs of cystourethroscopic videos were obtained before and four weeks after administration of alpha-1 blocker from 16 patients with BPH.

Eight pairs of cystourethroscopy were performed with a flexible video endoscope (CYF-VA2, Olympus Corp., Japan), and the other pairs were performed with a rigid scope (A2201A, Olympus Corp., Japan). The outer diameter of the scope was 16 Fr (5.3 mm), which means the morphological expansion of the urethra was driven by irrigation water pressure rather than the endoscope itself. Results of urine flow analysis were compared with parameters of voiding function obtained by conventional clinical examinations.

The 32 cystourethroscopic videos were recorded as an uncompressed AVI file with VGA resolution and processed into panoramic images using the method described in section II-A. Endoscope was operated manually by two skillful urologists after training for stable withdrawal maneuver. Hence, withdrawal velocity and axis of the movement of cystourethroscope included unavoidable perturbation. Stability of all cystourethroscopic videos were reviewed in terms of perimeter of the urethra are recorded and absence of stopped point in the video stream. Streams that are not satisfactory to the review were rejected before processing. Variance of water pressure around 20 cmH_2O may be also included following fall of water level of irrigant placed at 80 cm height from the urethral outlet. Seeing the scope withdrawing time was 10 seconds, the change of water pressure could be considered as minimal. Ten videos from five subjects were not suitable for generating panoramic images for the CFD analysis due to severe hypertrophy of the prostate or the presence of obstacles in the images, such as air bubbles or opaque liquid. Therefore, 11 pairs of cystourethroscopic videos were used for modeling the urethral shape and CFD analysis. To adjust the length of the 3D intra-urethral model in each pair of video files before and after alpha-1 blocker administration, panoramic images was processed and landmarks at the bladder outlet and verumontanum was overlaid in each pair of the image. Before the CFD calculation, the generated 3D model was processed two times using a 5 × 5 median filter and 5 × 5 moving-average filter for removing outliers and smoothing rough shapes caused by non-uniform blood vessel distribution. To follow the turbulent flow in the prostatic urethral model, the outlet side of the model for calculation was extended with the same cross-sectional shape. Preprocessing settings and boundary conditions were identical to those described in section II-B.

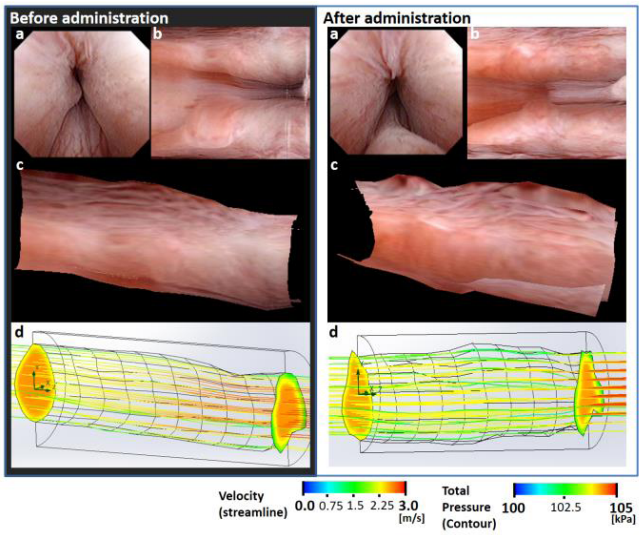

FIGURE 2. Visualization of simulated urine flow by the proposed method. Left: before; Right: after administration of an alpha-1 blocker. a: cystourethroscopic image; b: opened panoramic image; c: 3D urethral model; d: simulated streamline (with velocity color map) and contour of total pressure at inlet and outlet of the model. The flow direction is rightward of each figure. ΔP of two models were 310.9 Pa (before Tx.) and 241.3 Pa (after Tx.), respectively, and PLIR was 0.22.

After the CFD calculation, the streamline of each urine flow was visualized (Fig. 2). Turbulent flow and low flow velocity regions were observed in cases before alpha-1 blocker administration, while after administration, the turbulence were eliminated or reduced due to expansion of the urethra by smooth muscle relaxation. Turbulent flow was generated after the prostate obstruction, incrementing energy loss of urinary flow.

To evaluate the calculated parameters from the proposed method for clinical application, the pressure transition from the calculated values and indices from conventional clinical examinations were compared. Among conventional parameters of voiding function, prostate volume (*PV*), the international prostatic symptom score (*IPSS*), maximum flow rate (*Qmax*), *RU*, and differential values of these indices around administration of alpha-1 blocker ($\Delta IPSS$, $\Delta Qmax$ and ΔRU) were used. *PV* was estimated with a common clinical procedure by measuring width, length and height of

the prostate with ultrasonography [18]. *PV* directly affects the properties of the prostatic urethra on urine transportation. *IPSS* is widely used to estimate patients' complaints of lower urinary tract symptoms, ultimately indicating deterioration of patients' QOL. *Qmax* and *RU* are objective parameters that indicate the impulse of urine flow and volume of indwelling residual urine after micturition. *RU* is measured by ultrasonographic scanning of the bladder.

In 11 subjects, the mean ± SD of *PV, IPSS, Qmax* and *RU* before administration of the alpha-1 blocker were 36.6 ± 18.1 ml, 13.7 ± 7.9, 11.8 ± 4.9 ml/sec, and 36.3 ± 24.6 ml, respectively. After alpha-1 blocker administration, significant improvement was observed in *IPSS* and *Qmax* to be 7.0 ± 3.3 (p=0.0125), 16.6 ± 3.2 ml/min (p=0.0076), respectively. *RU* also improved to 27.0 ± 29.2 ml.

According to the proposed method, the total pressure loss between the inlet and outlet (ΔP) of each model also improved from 446.7 ± 214.3 Pa to 393.6 ± 176.1 Pa around the administration, providing *PLIR* to be 0.03 ± 0.41.

Besides, correlations among conventional and proposed indices were tested. Among the conventional indices, relationship was observed between *IPSS* before administration and *PV* (ρ=0.64, p=0.0325) and Δ*IPSS* and Δ*Qmax* (ρ=0.64, p=0.0331). *RU* revealed no relationship with IPSS (ρ=0.22). Then, the correlation between conventional indices and that of CFD analysis were compared. Relationship was observed between ΔP before alpha-1 blocker administration and *PV* (ρ=0.64, p=0.0353, Fig. 3), and *PLIR* and *RU* before administration (ρ=0.79, p=0.0038, Fig. 4). Though not significant, *PLIR* interestingly showed positive relationship with Δ*Qmax*, (ρ=0.36) and negative relationship with Δ*RU* (ρ=−0.39). Thus, it would be likely that *PLIR* reflect clinical symptoms, and should be estimated further using much more samples with better quality of video image.

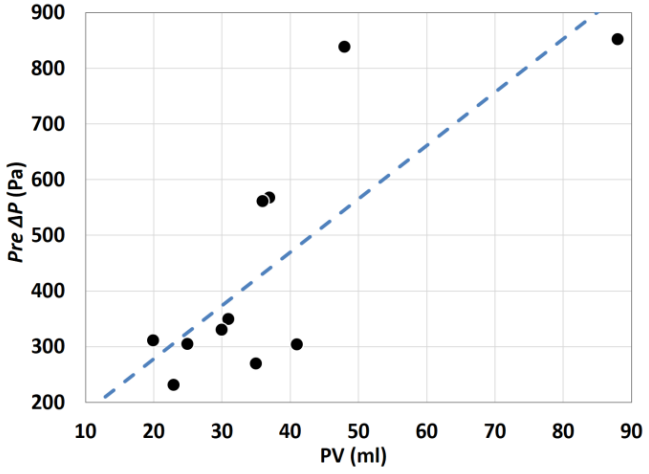

FIGURE 3. Relationship between prostate volume and ΔP before alpha-1 blocker administration. The pressure loss through the constructed urethral model correlated to the prostatic obstruction (ρ = 0.64).

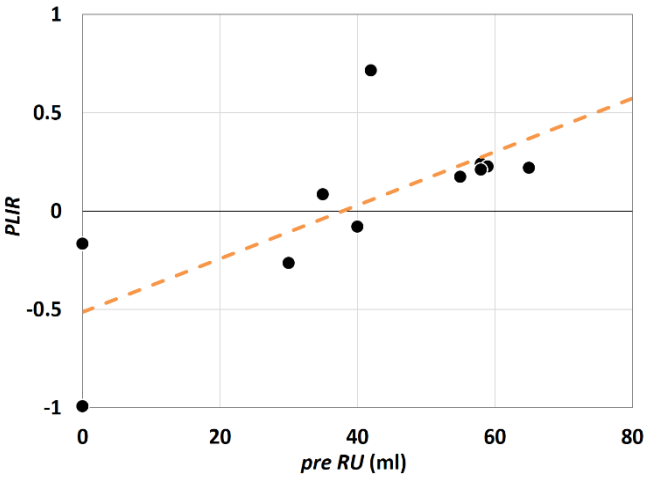

FIGURE 4. Relationship between RU before alpha-1 blocker administration (pre RU) and *PLIR*. The *PLIR* significantly corresponded to pre RU. (ρ = 0.79).

IV. DISCUSSION

There are currently various therapeutic modalities for managing voiding dysfunction. However, selecting the optimal method largely depends on a doctor's experience, except in patients with urinary retention [23], and therapeutic outcome often is difficult to foresee. The guidelines for male lower urinary tract symptoms published by the European Association of Urology in 2012 [24] recommend four types of alpha-1 blocker. Each type of blocker effects different subtypes of the alpha-1 adrenoceptor, and each subtype distributes differently in the urethral tissue [25]. Thus, alpha-1 blockers have different characteristics that affect dilation of the urinary tract during voiding. Complete resection of prostatic adenoma yields fair improvement of voiding function at the expense of deterioration of sexual function [26]–[28]. These problems are attributable to poor attention paid to the shape of the urethra in each patient for designing the optimal treatment.

It is intriguing to shed light on the fluid dynamics aspect of urine flow, where lower urinary tract symptoms are attributable to loss of hydraulic energy of the urine stream during passage through the urethra. Tojo et al. [14] and Yamanishi et al. [15] reported that the hydraulic energy loss of the urine flow in the urethra of patients with BPH is significantly larger than those without voiding dysfunction. Sakuyama et al. [17], [20] and Kambara et al. [16], [22] designed multiple urinary tract models representing BPH, BOO and other possible changes with lower urinary tract symptoms, and indicated that the pressure loss was caused at narrow points followed by substantial dilation in the urethra by generating vortices of urine flow.

In this study, we made attempt to evaluate the efficiency of the urine transport in the prostatic urethra by computing ΔP and *PLIR* in patients with voiding dysfunction. Since lack of optimal parameters that indicate deterioration of urine flow in the urethra, conventional voiding parameters were used as surrogates to validate the results of the proposed method.

IEEE Journal of Translational Engineering in Health and Medicine

As a result, ΔP before alpha-1 blocker administration corresponded to *PV*, but not to *IPSS*, *QOL*, *Qmax*, or *RU*. Seeing enlargement of the prostate directly affects alteration of property of the prostatic urethra by elongation or deformation, ΔP and *PV* is considered to be adequate indicator of local resistance of urine passage in the prostatic urethra. The assumption could be fortified by the no relationship between ΔP and the other voiding parameters that are integration of various factors including urethral deformation and neuro-muscular function.

PLIR is a chronological comparison of pressure loss in each patient around alpha-1 blocker administration. So, reproducibility of voiding parameters are decisive for statistical calculation. *RU* is considered to be reliable in spite of some fluctuation, and showed relationship with *PLIR*. In 2007, Shafik et al. reported interesting experiment that exertion of the urethral pressure at the external urethral sphincter provoked bladder contraction, suggesting pressure at this site facilitate voiding reflex [29]. The present study showed data compatible to the report that improved pressure at the distal part of the prostatic urethra would boost continuation of the voiding reflex, resulting in reduction of *RU*. Weak correlation between *PLIR* and improvement of *Qmax* could be attributable to the different voiding volume on examination in some patients that surely disturbed the data.

Since administration of alpha-1 blockers do not affect *PV* or detrusor contractility, the difference in ΔP around alpha-1 blocker administration is affected by the hydraulic energy loss in accordance with the alteration in the shape of the urethra. Therefore, the calculated fluid pressure transitions through the urethral model by the proposed method could estimate the ability of the prostatic urethra in transporting urine in individual patients.

As one of limitations of the proposed model construction, the algorithm of modeling could not reproduce the slight curvature of the prostatic urethra accurately by regarding the tubular axis as straight. As a result, the present study failed to calculate the possible curvature loss. Similarly, we used the same constants for maximum and minimum diameter and length of the urethral models for all subject. Calculating these parameters individually for each patients would afford to reproduce accurate shape of the prostatic urethra, and depict pressure distribution in the urethra more precisely. To overcome these problems, integration with tracking the position and posture of the tip of endoscope would be an essential solution. In addition, as we mentioned in section I, the modeling assumption would include depth distortion. Consequently, the reproducibility of the luminal shape would decrease when the actual shape was far from perfect cylinder, such as triangular shape at bladder outlet, and further study is mandatory in this respect. Besides, method of fluid dynamic computation used non-deformed model with steady flow, which is quite different from normal micturition that urethra expands by dynamic pressure of the unsteady urine flow. To reproduce approximately normal micturition, research using coupled analysis has been preparing to compare the data of present study. Since the proposed method is aimed for clinical application with timeliness, the results of the research would compensate the present method.

Comprehending the entire shape of the prostatic urethra and the behavior of urine flow through the tract with a sequence of cystourethroscopic images recorded with an optimal angle of view and depth cue served as a useful tool for calculating the intraluminal urine flow. Further, the visualization of urine flow in the prostatic urethra could indicate the location of possible lesions causing a loss of redundant fluid energy by depicting turbulence of flow, and would be a useful guide for determining optimal, less invasive pharmaceutical and surgical therapies. Thus, cystourethroscopy together with image processing would provide novel parameters to evaluate the expected effect of multiple types of drugs, and therapeutic modalities, such as resecting the urethral tissue lesions responsible for voiding dysfunction to dilate the urinary tract physically, by showing the expected deformation of the urethra after therapy.

To date, the treatment for voiding dysfunction is clinically evaluated by indirect parameters, such as observing changes in subjective scoring, as in *IPSS* and UDS at the outlet of the urethra. However, subjective scoring tends to be contingent on patients' characteristics, such as the baseline of the voiding quality and disease duration, while objective scoring may not reproduce patients' daily performance due to the unusual examination environment. In cases of the present study, $\Delta IPSS$ was corresponded to improvement of *Qmax*, however, relationship between $\Delta IPSS$ and ΔRU was very weak. The proposed indices revealed similar tendency of relationship and seemed to be better indicator for *RU*. Thus, *PLIR* would be another indicator for improvement of the symptoms of patients with BPH, comparable to the conventional parameters. Compared with conventional examinations for voiding dysfunction, the proposed method requires a sequence of cystourethroscopic images, which is already acquired in the routine clinical test, and supplies direct observation of urethral tissue while avoiding effects of physiological and psychological stress on the patient. The method would provide indices that represent urethral resistance to urine flow and therapeutic effects from an endoscopic video stream; however, a study with data from a large number of patients would be required to confirm the clinical validity. In the future, simulated urine flow behavior and dynamics with a personal urethral model will support personalized medication and treatment planning for patients with voiding dysfunction.

V. CONCLUSIONS

Using cystourethroscopic images of voiding dysfunction, urethral tissue modeling and determining the urethral shape to estimate efficiency of urine flow transportation in the prostatic urethra was proposed. Observation of shape and texture of the luminal organ and urine fluid dynamics such as pressure transition and streamline could be obtained using the proposed method, a prostatic urethral model with simulations, for evaluating voiding dysfunction.

The proposed method can provide detailed information on determining critical lesions to reduce the urine flow energy and urine flow behavior around the lesion with a 3D personalized urethral model, which will further support effective drug selection and help determine the most effective location and extent of resection in surgical planning, with the eventual goal of personalized medicine.

ACKNOWLEDGMENT

The authors would like to thank Dr. Kazuyoshi Nakamura and Dr. Tomokazu Sazuka for the cystourethroscopic images of patients with BPH.

REFERENCES

[1] K. S. Cho, J. Kim, Y. D. Choi, J. H. Kim, and S. J. Hong, "The overlooked cause of benign prostatic hyperplasia: Prostatic urethral angulation," *Med Hypotheses*, vol. 70, no. 3, pp. 532–535, 2008.

[2] W. J. Bang *et al.*, "Prostatic urethral angulation associated with urinary flow rate and urinary symptom scores in men with lower urinary tract symptoms," *Urology*, vol. 80, pp. 1333–1337, Dec. 2012.

[3] P. Glemain, J. M. Buzelin, and J. P. Cordonnier, "New urodynamic model to explain micturition disorders in benign prostatic hyperplasia patients. Pressure-flow relationships in collapsable tubes, hydraulic analysis of the urethra and evaluation of urethral resistance," *Eur. Urol.*, vol. 24, no. 1, pp. 12–17, 1993.

[4] A. W. El-Kassaby, T. Osman, A. Abdel-Aal, M. Sadek, and N. Nayef, "Dynamic three-dimensional spiral computed tomographic cysto-urethrography: A novel technique for evaluating post-traumatic posterior urethral defects," *BJU Int.*, vol. 92, pp. 993–996, Dec. 2003.

[5] R. K. Gupta, R. Kapoor, H. Poptani, H. Rastogi, and R. B. Gujral, "Cine MR voiding cystourethrogram in adult normal males," *Magn. Reson. Imag.*, vol. 10, no. 6, pp. 881–885, 1992.

[6] J. Ryu and B. Kim, "MR imaging of the male and female urethra," *Radiographics*, vol. 21, pp. 1169–1185, Sep./Oct. 2001.

[7] Y. Y. Ding, H. Ozawa, T. Yokoyama, Y. Nasu, M. B. Chancellor, and H. Kumon, "Reliability of color Doppler ultrasound urodynamics in the evaluation of bladder outlet obstruction," *Urology*, vol. 56, pp. 967–971, Dec. 2000.

[8] C. Duran, J. del Riego, L. Riera, C. Martin, C. Serrano, and P. Palana, "Voiding urosonography including urethrosonography: High-quality examinations with an optimised procedure using a second-generation US contrast agent," *Pediatric Radiol.*, vol. 42, pp. 660–667, Jun. 2012.

[9] T. Igarashi, S. Zenbutsu, T. Yamanishi, and Y. Naya, "Three-dimensional image processing system for the ureter and urethra using endoscopic video," *J. Endourol.*, vol. 22, pp. 1569–1572, Aug. 2008.

[10] T. Igarashi, S. Zenbutsu, Y. Naya, T. Ishii, W.-W. Yu, and T. Yamanishi, "Assessment of voiding function by endoscopic imaging—A preliminary report," *J. Mech. Med. Biol.*, vol. 9, no. 4, pp. 609–620, 2009.

[11] T. Igarashi and S. Zenbutsu, "Three-dimentional image forming device, three-dimensional image forming method and program," U.S. Patent 8 562 182, Jan. 1, 2009.

[12] T. Ishii, S. Zenbutsu, T. Nakaguchi, M. Sekine, Y. Naya, and T. Igarashi, "Novel points of view for endoscopy: Panoramized intraluminal opened image and 3D shape reconstruction," *J. Med. Imag. Health Inf.*, vol. 1, no. 1, pp. 13–20, 2011.

[13] T. Ishii, S. Zenbutsu, and T. Igarashi, "Modeling method of the male urethra from endoscopic imagery toward the least invasive surgery for patients with voiding dysfunction," in *Proc. 24th Int. Conf. Soc. Med. Innov. Technol.*, Barcelona, Spain, Sep. 2012, no. O-72.

[14] M. Tojo, K. Yasuda, T. Yamanishi, T. Hattori, K. Nagashima, and J. Shimazaki, "Relationship between bladder neck diameter and hydraulic energy at maximum flow," *J. Urol.*, vol. 152, no. 1, pp. 144–149, 1994.

[15] T. Yamanishi, K. Yasuda, R. Sakakibara, T. Hattori, and M. Tojo, "The effectiveness of terazosin, an alpha1-blocker, on bladder neck obstruction as assessed by urodynamic hydraulic energy," *BJU Int.*, vol. 85, no. 3, pp. 249–253, 2000.

[16] Y. Kambara *et al.*, "Visualization of 3D structure of the prostatic urethra and hydrodynamic simulation are valid for estimating LUTS in BPH patients," in *Proc. 41st Annu. Meeting Int. Continence Soc.*, Glasgow, U.K., 2011.

[17] G. Sakuyama, T. Ishii, Y. Naya, T. Yamanishi, and T. Igarashi, "A fluid dynamic model matched for voiding dysfunction in bladder outlet obstruction," *Urology*, vol. 76, no. 3, pp. S23–S24, 2010.

[18] K. M. Kalkner, G. Kubicek, J. Nilsson, M. Lundell, S. Levitt, and S. Nilsson, "Prostate volume determination: Differential volume measurements comparing CT and TRUS," *Radiotherapy Oncol.*, vol. 81, no. 2, pp. 179–83, Nov. 2006.

[19] *FloEFD Technical Reference*, Menter Graphics Corporation, Wilsonville, OR, USA, 2010.

[20] G. Sakuyama, T. Ishii, T. Yamanishi, and T. Igarashi, "Hydrodynamic aspects of intravesical protrusion of the prostate in patients with voiding dysfunction," *Urology*, vol. 78, no. 3, p. S94, 2011.

[21] H. P. Dietz and B. Clarke, "The urethral pressure profile and ultrasound imaging of the lower urinary tract," *Int. Urogynecol. J.*, vol. 12, no. 1, pp. 38–41, 2001.

[22] T. Ishii, Y. Naya, T. Yamanishi, and T. Igarashi, "Urine flow dynamics through the urethra in patients with bladder outlet obstruction," *J. Mech. Med. Biol.*, Oct. 2013, to be published.

[23] J. R. Wilson, G. H. Urwin, and M. J. Stower, "The changing practice of transurethral prostatectomy: A comparison of cases performed in 1990 and 2000," *Ann. Roy. College Surgeons England*, vol. 86, no. 6, pp. 428–431, Nov. 2004.

[24] M. Oelke *et al.*, "EAU guidelines on the treatment and follow-up of non-neurogenic male lower urinary tract symptoms including benign prostatic obstruction," *Eur. Urol.*, vol. 64, pp. 118–140, 2013.

[25] S. Yamada and Y. Ito, "α(1)-adrenoceptors in the urinary tract," *Handbook Experim. Pharmacol.*, vol. 1, no. 1, pp. 283–306, 2011.

[26] M. Muntener, S. Aellig, R. Kuettel, C. Gehrlach, T. Sulser, and R. T. Strebel, "Sexual function after transurethral resection of the prostate (TURP): Results of an independent prospective multicentre assessment of outcome," *Eur. Urol.*, vol. 52, pp. 510–515, Aug. 2007.

[27] F. Bruyere, "The relationship between photoselective vaporization of the prostate and sexual function," *Current Urol. Rep.*, vol. 12, pp. 261–264, Aug. 2011.

[28] A. Kumar, P. Vasudeva, N. Kumar, B. Nanda, and N. K. Mohanty, "Evaluation of the effect of photoselective vaporization of the prostate on sexual function in a prospective study: A single center experience of 150 patients," *J. Endourol.*, vol. 26, pp. 11–15, Oct. 2012.

[29] A. Shafik, I. A. Shafik, O. El Sibai, and A. A. Shafik, "Effect of urethral stimulation on vesical contractile activity," *Amer. J. Med. Sci.*, vol. 334, no. 4, pp. 240–243, Oct. 2007.

TAKURO ISHII (S'01) received the B.Sc. and M.Sc. degrees in engineering from Chiba University, Chiba, Japan, in 2009 and 2011, respectively, where he is currently pursuing the Degree with the Department of Medical System, Graduate School of Engineering.

He has been a Research Fellow of the Japan Society for the Promotion of Science since 2012. His research interests include image processing for endoscopic images, in particular, spatial recognition of body cavity for medical staffs and fluid dynamics analysis in lower urinary tract.

YOICHI KAMBARA received the B.Sc. and M.Sc. degrees in engineering from Chiba University, Chiba, Japan, in 2011 and 2013, respectively.

His research topics are shape modeling of urinary tract and urine flow analysis for voiding dysfunction.

IEEE Journal of Translational Engineering in Health and Medicine

TOMONORI YAMANISHI received the bachelor's and medical degrees from the Chiba University School of Medicine, Chiba, Japan, in 1982, where he served as an Assistant Professor with the Department of Urology from 1989 to 1997, and then a Lecturer until 2001. He was with the Department of Urology and the Department of Biomedical Science, University of Sheffield, U.K., from 1998 to 2001. After completing his studies at the University of Sheffield, he returned to Japan in 2001 and was with the Urology Department, Dokkyo Medical University, Tochigi, Japan, as an Associate Professor.

He has been a Professor of Urology, Dokkyo Medical University, since 2009, where he was the Chief of Continence Center in 2011.

Prof. Yamanishi is a Boarding Member of the Japanese Urological Association, Japanese Neurogenic Bladder Society, Japan Medical Association of Spinal Cord Lesion, and Japanese Association of Enuresis, and also a member of the International Continence Society, European Association of Urology, American Urological Association, International Spinal Cord Society, and International Urogynecological Association.

YUKIO NAYA received the M.D. and Ph.D. degrees from the Faculty of Medicine, Chiba University, Chiba, Japan.

He has served as a Urologist at the Yokohama Rosai Hospital for nine years after graduation, and has started academic activity at Chiba University since 2000, then he joined the Department of Urology, Teikyo University, as a Professor, in 2010.

He is a top-ranked surgeon in Japan, in particular, the urological field. His research interest is laparoscopic surgery for the urogenital organs and endourology, in particular, establishment of focal therapy in the urological field.

TATSUO IGARASHI received the M.D. and Ph.D. degrees from the Faculty of Medicine, Chiba University, Chiba, Japan, in 1985. He served as a Urologist with the Asahi General Hospital, Chiba, from 1984 to 1998, resumed to academic activity as an Associate Professor with the Department of Urology, Chiba University, then moved to the Research Center for Frontier Medical Engineering as a Professor in 2003. His research interest is endoscopic image processing and macroscopic flow dynamics in the body cavity, in particular, the novel surgical system carried out under water.